

γ -Amino butyric acid analogs as novel potent GABA-AT inhibitors: molecular docking, synthesis, and biological evaluation

S. K. Bansal · B. N. Sinha · R. L. Khosa

Received: 8 December 2011 / Accepted: 7 March 2012 / Published online: 20 March 2012
© Springer Science+Business Media, LLC 2012

Abstract A new series, of γ -amino butyric acid analogs were designed and synthesized as novel potent GABA-AT inhibitors. A structure–activity relationship study was performed by correlating the effect of different substituents with GABA-AT inhibitory activity of the title compounds. The preliminary bioassays showed that acid hydrazones exhibited excellent inhibitory activities in micromolar (0.07–0.56 μ M) range, while Schiff's bases showed variable results. The most potent compound, 4-amino-*N'*-[(1*Z*)-1-(2-bromophenyl)ethylidene]butanehydrazide (AHG177) showed inhibitory potency (IC_{50}) of 0.073 μ M. Aminobutyrate transaminase is a pyridoxal-P enzyme which follows a bi–bi ping pong mechanism and in pyridoxamine form can readily transaminate only with succinic semialdehyde and 2-oxoglutarate. The results strongly suggest that only the pyridoxal form of the enzyme is capable of reacting with the ligands. Our findings open up the possibility to extend this protocol to different databases in order to find new potential inhibitor for promising targets based on a rational drug design process.

Keywords AutoDock 4.0.1 · Docking simulation · GABA · GABA-AT inhibitor · IC_{50} · Lamarckian genetic algorithm

Introduction

The search for antiepileptic compounds with a more selective activity and lower toxicity continues to be an area of investigation in medicinal chemistry. A rational drug design process of a new anticonvulsant could be achieved by the identification of new targets through better understanding of molecular mechanisms of epilepsy. Novel anticonvulsant agents are discovered through conventional screening and/or structure modification rather than a mechanism-driven design (Barbara, 2005). Docking-based drug design by the use of structural biology remains one of the most logical and aesthetically pleasing approaches in drug discovery paradigms. The structured knowledge of the binding capabilities of the active site residues to specific groups on the agonist or antagonist leads to proposals for synthesis of very specific agents, with a high probability of biological action (Hardy *et al.*, 2003).

Virtual screening of compound libraries has become a standard technology in modern drug discovery pipelines. If a suitable structure of the target is available, molecular docking can be used to discriminate between putative binders and non-binders in large databases of chemicals and to reduce the number of compounds to be subjected to experimental testing substantially. Molecular docking is one of the key computational chemistry techniques that are routinely applied to drug discovery. The holy grail of molecular docking is to replace experimental studies of protein ligand complexes by modelling their structures and binding affinities *in silico* (Novikov and Chilov, 2009)

Electronic supplementary material The online version of this article (doi:10.1007/s00044-012-0023-0) contains supplementary material, which is available to authorized users.

S. K. Bansal (✉) · R. L. Khosa
Department of Medicinal Chemistry, School of Pharmacy,
Bharat Institute of Technology, Meerut 250103, UP, India
e-mail: skbansal@bitmeerut.edu.in; skbansal2003@gmail.com

B. N. Sinha
Division of Molecular Modelling, Department of Pharmaceutical
Sciences, Birla Institute of Technology, Mesra, Ranchi 835215,
Jharkhand, India

γ -Amino butyric acid (GABA) is a predominant inhibitory neurotransmitter in mammalian CNS modulating central inhibitory tone via activation of ionotropic GABA_A and GABA_C receptor and G-Protein-coupled GABA_B receptor (Osolodkin *et al.*, 2009; Smith and Simpson, 2003). γ -Amino butyrate aminotransferase (GABA-AT) catalyzes the degradation of GABA to succinic semialdehyde (SSA). Depleted levels of GABA have been shown to cause convulsions (Karlsson *et al.*, 1974). Raising GABA levels in brain have an anticonvulsive effect (Krogsgaard-Larsen, 1981). GABA-AT is a validated target for antiepileptic drugs because its selective inhibition raises GABA concentration in brain (Storici *et al.*, 1999). Numerous strategies exist to elevate GABA levels in the brain. The strategy, which we have taken, involves the inhibition or the inactivation of GABA-AT (Bansal *et al.*, 2010, 2011a, b, c; Nogardy and Weaver, 2005; Silverman and Clift, 2008; Sowa *et al.*, 2005). GABA itself is not an effective anticonvulsive agent since it does not cross the blood brain barrier, a protective membrane that prevents xenobiotics from entering the brain (Silverman *et al.*, 1986). Consequently, a real need exists to develop new anticonvulsant compounds to cover seizures which are so far resistant to presently available drugs. Current marketed antiepileptic drugs consist of a variety of structural classes (lamotrigine, oxcarbazepine, topiramate, gabapentin, and levetiracetam) with different mechanisms of action. These agents typically have non-overlapping efficacy and side effect profiles presenting multiple treatment options for the patient population. However, approximately 30 % of seizure sufferers fail to respond to current therapies. Currently, there is no single drug of choice for treating all types of seizures. One should focus on mechanism-driven discovery of novel compounds followed by their evaluation by *in vitro* and *in vivo* models to discover novel antiepileptic drugs. Several recent successes (pregabalin, brivaracetam) have shown that knowledge of the mechanism of action gives the developer a significant advantage in improving efficacy through increased target potency and selectivity, thereby lowering the potential for dose-related side effects. It is the hope that new generation AEDs with novel mechanisms will increase the likelihood for success in treating a heterogeneous patient population (Gerlach and Krajewski, 2010).

A strategy along this line is to search for compounds with new modes of action, a series of GABA with an imine link to a wide variety of alkyl and aryl aldehydes, ketones has been designed, synthesized, and screened

In this study, our goal was to apply computational techniques in the pursuit of potential inhibitors of GABA-AT enzyme activity. Molecular docking simulations were employed to both find hit compounds and to rank the best fit of the ligands.

Materials and methods

GABA-AT receptor modeling

The receptor model was prepared using AutoDock Tools[®] 1.4.6 and MGL Tools[®] 1.5.4 packages (The Scripps Research Institute, Molecular Graphics Laboratory, 10550 North Torrey Pines Road, CA, 92037) running on Red Hat Enterprise Linux 5.0.

It consists of several steps. First, the 3D crystal structure of GABA-AT; PDB code 1OHV (Kwon *et al.*, 1992; Storici *et al.*, 2005; Toney *et al.*, 1995) was downloaded from Brookhaven protein data bank (PDB; <http://www.rcsb.org/pdb>) and loaded to python molecular viewer. The non-bonded oxygen atoms of waters, present in the crystal structure were removed. After assigning the bond orders, missing hydrogen atoms were added, then the partial atomic charges was calculated using Gasteiger–Marsili (1980) method. Kollman and co-workers (1984) united atom charges were assigned, non-polar hydrogens merged and rotatable bonds were assigned, considering all the amide bonds as non-rotatable. The receptor file was converted to pdbqt format, which is pdb plus “q” charges and “t” AutoDock type. (To confirm to the AutoDock types, polar hydrogens should be present where as non-polar hydrogens and lone pair should be merged, each atom should be assigned Gasteiger partial charges).

Since vigabatrin (Fig. 1) forms a covalent ternary adduct with the active site LYS 329 (22) of GABA-AT, therefore LYS 329 was included as flexible residue for introducing conformational search of flexible side chain. For the same macromolecule was saved in two files: one containing the formatted, flexible LYS 329 residue, and the other all the rest of the residues in the macromolecule.

Ligand modeling

ChemDraw Ultra 6.0.1 (Cambridge Soft.Com, 100 Cambridge park drive, Cambridge, MA 02140, USA) was used to draw the 3D structures of different ligands (Schiff's bases of GABA). Ligands were further refined and cleaned in 3D by addition of explicit hydrogens and gradient optimization function of MarvinSketch 5.0.6.1 (Chemaxon Ltd; <http://www.Chemaxon.com>). All the structures were written in Tripos mol2 file format.

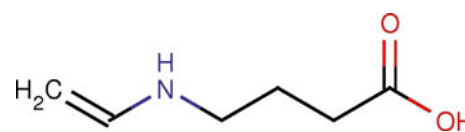


Fig. 1 Chemical structure of vigabatrin

Input molecules files for an AutoDock experiments must confirm to the set of atom types supported by it. AutoDock requires that, ligands give partial atomic charges and AutoDock atom types for each atom; it also requires a description of the rotatable bond in the ligand. AutoDock uses the idea of a tree in which the rigid core of the molecule is a “root,” and the flexible parts are “branches” that emanate from the root. This set consists of united atom aliphatic carbons, aromatic carbons in cycles, polar hydrogens, hydrogen-bonded nitrogen, and directly hydrogen-bonded oxygen among others, each with partial charges. Therefore, pdbqt format was used to write ligands, recognized by AutoDock.

Torsional degree of freedom (TORSDOF) is used in calculating the change in the free energy caused by the loss of TORSDOF upon binding. In the AutoDock 4.0.1 force field, the TORSDOF value for a ligand is the total number of rotatable bonds in the ligand. This number excludes bonds in rings, bonds to leaf atoms, amide bonds, and guanidinium bonds.

Molecular docking simulations

Prior to actual docking run, AutoGrid 4.0.1, was introduced to pre-calculate grid maps of interaction energies of various atom types (Goodford, 1985). In all dockings, a grid map with $60 \times 60 \times 60$ points, a grid spacing of 0.375 \AA (roughly a quarter of the length of a carbon–carbon single bond) were used, and the maps were centered on the ligand binding site. In an AutoGrid procedure, the protein is embedded in a 3D grid and a probe atom is placed at each grid point. The energy of interaction of this single atom with the protein is assigned to the grid point. An affinity grid is calculated for each type of atoms in the substrate, typically carbon, oxygen, nitrogen, and hydrogens as well as grid of electrostatic potential using a point charge of +1 as the probe (Allison *et al.*, 1998; Sharp *et al.*, 1987). AutoDock 4.0.1 uses these interaction maps to generate ensemble of low energy conformations (Goodsell and Olson, 1990; Morris *et al.*, 1996). It uses a scoring function based on AMBER force field, and estimates the free energy of binding of a ligand to its target. For each ligand atom types, the interaction energy between the ligand atom and the receptor is calculated for the entire binding site which is discretized through a grid. This has the advantage that interaction energies do not have to be calculated at each step of the docking process but only looked up in the respective grid maps. Since a grid map represents the interaction energy as a function of the coordinates, their visual inspection may reveal the potential unsaturated hydrogen acceptors or donors or unfavorable overlaps between the ligand and the receptor.

Of the three different search algorithms offered by AutoDock 4.0.1, the Lamarckian genetic algorithm (LGA) based on the optimization algorithm (Solis and Wets, 1981)

was used, since preliminary experiments using other two (simulated annealing and genetic algorithm) showed that they are less efficient, utilizes (discredited) Lamarckian notation that an adaptations of an individual to its environment can be inherited by its offspring. For all dockings, 100 independent runs with step sizes of 0.2 \AA for translations and 5 \AA for orientations and torsions, an initial population of random individuals with a population size of 150 individuals, a maximum number of 2.5×10^6 energy evaluations, maximum number of generations of 27,000, an elitism value of 1, a number of active torsion of 9 were used.

AutoDock Tools[®] along with AutoDock 4.0.1 and AutoGrid 4.0.1 was used to generate both grid and docking parameter files (i.e., gpf and dpf files), respectively.

Chemistry

All reagents obtained from commercial sources were analytical reagent grade. Melting points were determined in open capillary tubes on a Buchi melting point apparatus and are uncorrected.

Infrared (IR) spectra were obtained on a Perkin Elmer RX-1 FTIR spectrophotometer in the region $4,000\text{--}400 \text{ cm}^{-1}$ using KBr disc. Proton nuclear magnetic resonance (¹H NMR) spectra were recorded on Bruker ADVANCE-300 MHz using tetramethyl silane (TMS) as an internal standard and chemical shifts are reported in parts per million (ppm). Mass spectra were recorded on Shimadzu GCMS-QP1000EX. The progress of the reaction was monitored by ascending thin layer chromatography (TLC) on silica gel-G (Merck)-coated aluminum plates, visualized by iodine vapor and UV light. The eluant system was benzene:methanol (8:2). Homogeneity of the compounds was checked by TLC followed by high performance liquid chromatography (HPLC), WATERS-2489, using same eluant system.

General procedure for the synthesis of 4-amino-*N'*-aryl/alkylidenebutanehydrazide (**1–10**) and 3-amino-*N'*-aryl/alkylidenebenzohydrazide (**22–26**)

A solution of the amino acid (GABA/3-aminobenzoic acid; AA; 100 mmol) in a mixture of dioxane (20 ml), water (10 ml), and 1 M sodium hydroxide (10 ml) was stirred and cooled in ice water bath. Di-*t*-butyl pyrocarbonate (2.4 g, 110 mmol) was added and stirring was continued at room temperature for 30 min. The solution after acidification with dilute aqueous potassium hydrogen sulfate to pH 2–3 was extracted with ethyl acetate ($2 \times 15 \text{ ml}$). The ethyl acetate extracts were pooled, washed with water ($2 \times 30 \text{ ml}$), dried over anhydrous sodium sulfate and evaporated in vacuo. Recrystallization of the residue with

ethyl acetate–hexane offered the N-protected amino acids (BOC-AA). Equimolar quantities of BOC-AA (100 mmol) and hydrazine hydrate (99–100 %) (100 mmol) were condensed in the presence of dicyclohexylcarbodiimide (DCC) (100 mmol) in dichloromethane, by stirring at ice cold conditions (0–3 °C) for 7–9 h. The residue was filtered, washed, dried, recrystallized, and yielded BOC-AA-hydrazide. Imines were prepared by the reaction of BOC-AA-hydrazide (100 mmol) with different aldehydes and ketones (100 mmol) with the simultaneous removal of water (by the addition of glacial acetic acid) for 10–12 h. The BOC was removed by treatment of the different products with equimolar quantities of neat trifluoroacetic acid for 60 min. The final product was filtered, washed, dried, and recrystallized using suitable solvents and used further. The IR spectrum of 4-amino-*N'*-[aryl/alkyl-ylidene]butanehydrazide (**1–10**) and 3-amino-*N'*-aryl/alkylidenebenzohydrazide (**22–26**) showed the presence of peaks at 3,370 (OH of COOH), 1,700 (CO of COOH), 1,620–1,590 (C≡N) cm⁻¹.

¹H NMR (300 MHz, δ ppm) spectra and *m/z* of titled compounds are as follows:

4-Amino-N'-[1-(2-bromophenyl)ethylidene]butanehydrazide (**1**)

¹H NMR (300 MHz, DMSO): δ 0.855 (s, 3H, CH₃), 1.217–1.509 (m, 2H, CH₂ β to NH₂), 1.993 (s, 2H, NH₂, D₂O exchangeable), 2.196 (t, 2H, *J* = 12.3 Hz, CH₂ γ to NH₂), 2.767 (t, 2H, *J* = 9.3 Hz, CH₂ α to NH₂), 7.502–7.727 (m, 4H, aryl-H), 9.964 (s, H of CONH, D₂O exchangeable); MS (M+1)⁺ *m/z* = 298.9.

4-Amino-N'-[1-(3-chlorophenyl)ethylidene]butanehydrazide (**2**)

¹H NMR (300 MHz, DMSO): δ 0.735 (s, 3H, CH₃), 1.397–1.822 (m, 2H, CH₂ β to NH₂), 1.995 (s, 2H, NH₂, D₂O exchangeable), 2.254 (t, 2H, *J* = 6.3 Hz, CH₂ γ to NH₂), 2.781 (t, 2H, *J* = 6.6 Hz, CH₂ α to NH₂), 7.453–7.698 (m, 4H, aryl-H), 9.375 (s, H of CONH, D₂O exchangeable); MS (M+1)⁺ *m/z* = 254.5.

4-Amino-N'-[2-methyl-10-oxo-9,10-dihydroanthracene-9-ylidene]butanehydrazide (**3**)

¹H NMR (300 MHz, CDCl₃): δ 1.621–1.726 (m, 2H, CH₂ β to NH₂), 1.920 (s, 2H, NH₂, D₂O exchangeable), 2.252 (t, 2H, *J* = 8.1 Hz, CH₂ γ to NH₂), 2.569 (s, 3H, 2-CH₃ of 10-oxo-9,10-dihydroanthracene), 2.768 (t, 2H, *J* = 6.9 Hz, CH₂ α to NH₂), 7.261–7.782 (m, 7H, aryl-H), 9.822 (s, H of CONH, D₂O exchangeable); MS (M+1)⁺ *m/z* = 322.5.

4-Amino-N'-[3-iodophenylmethylidene]butanehydrazide (**4**)

¹H NMR (300 MHz, D₂O): δ 1.455–1.537 (m, 2H, CH₂ β to NH₂), 1.870 (t, 2H, *J* = 2.7 Hz, CH₂ γ to NH₂), 2.538 (t, 2H, *J* = 3.0 Hz, CH₂ α to NH₂), 6.769–8.018 (5H, aryl-H and HC=N); MS (M+1)⁺ *m/z* = 332.1.

4-Amino-N'-[1, 2, 3, 4-tetrahydronaphthalene-2-ylidene]butanehydrazide (**5**)

¹H NMR (300 MHz, CDCl₃): δ 1.818–2.056 (m, 6H, 3-CH₂ of naphthyl, CH₂ β to NH₂ and NH₂, D₂O exchangeable), 2.561–2.660 (m, 8H, CH₂ α , γ to NH₂ and 1,4-CH₂ of naphthyl), 7.268–8.770 (m, 4H, 5,6,7,8-CH of naphthyl), 9.129 (s, H of CONH, D₂O exchangeable); MS (M+1)⁺ *m/z* = 246.1.

4-Amino-N'-(10-oxo-9, 10-dihydroanthracene-9-ylidene)butanehydrazide (**6**)

¹H NMR (300 MHz, CDCl₃): δ 1.530–1.600 (m, 2H, CH₂ β to NH₂), 1.803 (s, 2H, NH₂, D₂O exchangeable), 2.142 (t, 2H, *J* = 8.4 Hz, CH₂ γ to NH₂), 2.649 (t, 2H, *J* = 8.4 Hz, CH₂ α to NH₂), 6.965–8.101 (m, 8H, aryl-H), 9.630 (s, H of CONH, D₂O exchangeable); MS (M+1)⁺ *m/z* = 308.6.

4-Amino-N'-[2-iodophenylmethylidene]butanehydrazide (**7**)

¹H NMR (300 MHz, DMSO): δ 1.257–1.342 (m, 2H, CH₂ β to NH₂), 1.600 (t, 2H, *J* = 5.1 Hz, CH₂ γ to NH₂), 2.058 (s, 2H, NH₂, D₂O exchangeable), 2.520 (t, 2H, *J* = 5.1 Hz, CH₂ α to NH₂), 7.522–8.038 (6H, aryl-H and HC=N), 9.003 (s, H of CONH, D₂O exchangeable); MS (M+1)⁺ *m/z* = 332.0.

4-Amino-N'-[1,2,3,4-tetrahydronaphthalen-1-ylidene]butanehydrazide (**8**)

¹H NMR (300 MHz, CDCl₃): δ 1.132–1.391 (m, 2H, 2-CH₂ of naphthyl), 1.730 (s, 2H, NH₂, D₂O exchangeable), 1.894–2.006 (m, 4H, 3-CH₂ of naphthyl and CH₂ β to NH₂), 2.597–2.719 (m, 6H, 4-CH₂ of naphthyl and CH₂ α , γ to NH₂), 7.196–7.876 (m, 4H, 5,6,7,8-CH of naphthyl), 8.721 (s, H of CONH, D₂O exchangeable); MS (M+1)⁺ *m/z* = 246.8.

4-Amino-N'-[2-oxo-1, 2-diphenylethylidene]butanehydrazide (**9**)

¹H NMR (300 MHz, DMSO): δ 1.540–1.630 (m, 2H, CH₂ β to NH₂), 2.091 (s, 2H, NH₂, D₂O exchangeable), 2.320 (t,

2H, $J = 10.8$ Hz, CH₂ γ to NH₂), 2.752 (t, 2H, $J = 8.1$ Hz, CH₂ α to NH₂), 7.094–8.372 (m, 10H, aryl-H), 9.081 (s, H of CONH, D₂O exchangeable); MS (M⁺) $m/z = 309.2$.

4-Amino-N'-[4-bromophenyl(phenyl)methylidene]butanehydrazide (10)

¹H NMR (300 MHz, DMSO): δ 1.671–1.804 (m, 2H, CH₂ β to NH₂), 1.908 (s, 2H, NH₂, D₂O exchangeable), 2.282 (t, 2H, $J = 5.4$ Hz, CH₂ γ to NH₂), 2.735 (t, 2H, $J = 7.2$ Hz, CH₂ α to NH₂), 6.780–8.225 (m, 9H, aryl-H), 9.096 (s, H of CONH, D₂O exchangeable); MS (M+1)⁺ $m/z = 360.4$.

3-Amino-N'-[1, 2-dihydroxy-10-oxo-9,10-dihydroanthracene-9-ylidene]benzohydrazide (22)

¹H NMR (300 MHz, CDCl₃): δ 4.164 (s, 2H, NH₂, D₂O exchangeable), 4.948 (s, 2H, 9,10-dihydroanthracene-1, 2-OH, D₂O exchangeable), 6.767–7.436 (m, 10H, aryl-H), 9.002 (s, H of CONHN, D₂O exchangeable); MS (M⁺) $m/z = 373.5$.

3-Amino-N'-[1-(3-chlorophenyl)ethylidene]benzohydrazide (23)

¹H NMR (300 MHz, CDCl₃): δ 0.859 (s, 3H, CH₃), 4.662 (s, 2H, NH₂, D₂O exchangeable), 6.761–7.410 (m, 8H, aryl-H), 8.009 (s, H of CONHN, D₂O exchangeable); MS (M+1)⁺ $m/z = 288.0$.

3-Amino-N'-[4-chlorophenyl(phenyl)methylidene]benzohydrazide (24)

¹H NMR (300 MHz, CDCl₃): δ 3.676 (s, 2H, NH₂, D₂O exchangeable), 6.716–8.073 (m, 13H, aryl-H), 8.184 (s, H of CONHN, D₂O exchangeable); MS (M⁺) $m/z = 349.0$

3-Amino-N'-[2-chloro-10-oxo-9,10-dihydroanthracene-9-ylidene]benzohydrazide (25)

¹H NMR (300 MHz, CDCl₃): δ 4.715 (s, 2H, NH₂, D₂O exchangeable), 6.771–7.462 (m, 13H, aryl-H), 8.655 (s, H of CONHN, D₂O exchangeable); MS (M⁺) $m/z = 375.0$

3-Amino-N'-(2,3,5,6-tetrachloro-4-oxocyclohexa-2,5-dien-1-ylidene)benzohydrazide (26)

¹H NMR (300 MHz, DMSO) δ 4.237 (s, 2H, NH₂, D₂O exchangeable), 6.937–7.385 (m, 4H, aryl-H), 8.403 (s, H of CONHN, D₂O exchangeable); MS (M+1)⁺ $m/z = 378.2$.

General procedure for the synthesis of 4-(aryl/alkylideneamino) butanoic acid (**11**, **13–21**) and 3-(aryl/alkylideneamino) benzoic acid (**27–31**)

To a suspension of amino acid (GABA/3-aminobenzoic acid; AA; 100 mmol) in absolute ethanol (80 ml) was added concentrated sulphuric acid (15 ml). The resulting yellow solution was heated at a reflux for 3 h, cooled to 0 °C and neutralized with concentrated aqueous ammonia solution. The precipitated product was then collected by filtration, washed with cold water, and recrystallized from aqueous ethanol to give pure amino acid ester. A mixture of amino acid ester (100 mmol), carbonyl compound (100 mmol), and catalytic amount of glacial acetic acid was added to absolute ethanol (60 ml). The mixture was refluxed for 4 h and cooled. The resultant precipitate was filtered off, washed with water (3 × 100 ml), dried over anhydrous magnesium sulfate. The resulted product was boiled with 80 ml of 10 % potassium hydroxide under reflux for 1 h and the liquid was distilled off through same condenser. Residue in the flask (potassium salt of product) was acidified with dilute sulphuric acid, separated product was filtered, washed water and, ethyl ether and dried over anhydrous magnesium sulfate. Recrystallization with alcohol and column purification led to the desired derivatives.

The IR spectrum of 4-(aryl/alkylideneamino)butanoic acid (**11**, **13–21**) and 3-(aryl/alkylideneamino)benzoic acid (**27–31**) showed the presence of peaks at 3,220 (NH stretching vibration), 1,650–1,630 (amide bond), 1,620–1,590 (C≡N) cm⁻¹.

¹H NMR (300 MHz, δ ppm) spectrum and m/z of titled compounds are as follows:

4-[[1,5-Diphenylpenta-1,4-dien-3-ylidene]amino]butanoic acid (11)

¹H NMR (300 MHz, CDCl₃): δ 0.850 (t, 2H, $J = 7.5$ Hz, CH₂ γ to COOH), 1.649–1.787 (m, 2H, CH₂ β to COOH), 2.515 (t, 2H, $J = 7.8$ Hz, CH₂ α to COOH), 5.785 (d, 2H, $J = 3.9$ Hz, diene-CH), 6.557–7.766 (m, 12H, aryl-H), 11.203 (s, 1H, COOH, D₂O exchangeable); MS (M+1)⁺ $m/z = 320.8$.

4-[[1,3,3-Trimethylbicyclo[2.2.1]heptan-2-ylidene]amino]butanoic acid (13)

¹H NMR (300 MHz, CDCl₃): δ 0.797 (d, $J = 5.4$ Hz, 3H, 1-CH₃), 0.903–0.935 (m, 8H, 1,3-CH₃ and CH₂ γ to COOH), 0.950–1.020 (m, 2H, 5-CH₂) 1.075–1.146 (m, 2H, 6-CH₂), 1.409–1.463 (m, 1H 4-CH), 1.587–1.682 (m, 2H, CH₂ β to COOH), 1.887–1.991 (m, 2H, bridged-CH₂), 2.148–2.224, 2.763–2.826 (m, 2H, CH₂ α to COOH),

10.455 (s, 1H, COOH, D₂O exchangeable); MS (M+1)⁺ *m/z* = 238.0.

4-[[10-Oxo-9,10-dihydrophenanthrene-9-ylidene]amino]butanoic acid (14)

¹H NMR (300 MHz, CDCl₃): δ 1.980–2.006 (m, 2H, CH₂ β to COOH), 2.231 (t, 2H, *J* = 3.3 Hz, CH₂ γ to COOH), 3.410 (t, 2H, *J* = 2.7 Hz, CH₂ α to COOH), 6.960–7.600 (m, 8H, aryl-H), 11.204 (s, 1H, COOH, D₂O exchangeable); MS (M⁺) *m/z* = 293.7.

4-[[2-Oxo-1, 2-dihydroacenaphthylene-1-ylidene]amino]butanoic acid (15)

¹H NMR (300 MHz, CDCl₃): δ 1.920–2.005 (m, 2H, CH₂ β to COOH), 2.320 (t, 2H, *J* = 6.9 Hz, CH₂ γ to COOH), 3.702 (t, 2H, *J* = 4.5 Hz, CH₂ α to COOH), 7.025–7.748 (m, 6H, aryl-H), 10.979 (s, 1H, COOH, D₂O exchangeable); MS (M+1)⁺ *m/z* = 268.8.

4-[[2-Methylcyclohexylidene]amino]butanoic acid (16)

¹H NMR (300 MHz, CDCl₃): δ 0.757–1.040 (m, 9H, 2-cyclohexyl-CH₃, CH₂ γ to COOH and 3,4-cyclohexyl-CH₂), 1.253–1.280 (m, 2H, 5-cyclohexyl-CH₂), 1.588–1.667 (m, 2H, CH₂ β to COOH), 1.917–2.695 (m, 5H, CH₂ α to COOH, 2-cyclohexyl-CH, 6-cyclohexyl-CH₂), 10.146 (s, 1H, COOH, D₂O exchangeable); MS (M+1)⁺ *m/z* = 198.1.

4-[[5-Methyl-2-(propan-2-yl)cyclohexylidene]amino]butanoic acid (17)

¹H NMR (300 MHz, DMSO): δ 0.790 (d, 9H, *J* = 32.6 Hz, 5-methyl-2-(propan-2-yl)), 1.256–1.314 (t, 2H, *J* = 8.7 Hz, CH₂ γ to COOH), 1.557 (t, 2H, *J* = 14.1 Hz, 4-cyclohexyl-CH₂), 1.940 (d, 2H, *J* = 13.2 Hz, 2,5-cyclohexyl-CH), 2.151–2.241 (m, 6H, CH₂ β to COOH, 3,5-cyclohexyl-CH₂), 2.751–2.754 (m, 3H, CH₂ α to COOH, propan-2-yl-CH), 9.752 (s, 1H, COOH, D₂O exchangeable); MS (M⁺) *m/z* = 239.2.

4-[[2-Methyl-5-(prop-1-en-2-yl)cyclohex-2-en-1-ylidene]amino]butanoic acid (18)

¹H NMR (300 MHz, D₂O): δ 1.226 (t, 2H, *J* = 6.6 Hz, 6-cyclohexyl-CH₂), 1.380 (t, 2H, *J* = 3.0 Hz, CH₂ γ to COOH), 1.475 (t, 2H, *J* = 3.6 Hz, 4-cyclohexyl-CH₂), 1.580–1.665 (m, 2H, CH₂ β to COOH), 1.842 (s, 6H, CH₃), 2.175 (t, 3H, *J* = 5.4 Hz, CH₂ α to COOH, 5-cyclohexyl-CH), 4.750 (s, 2H, 5-cyclohexyl-{1-prop-1-en-2-yl-CH₂}),

6.705–6.770 (m, 1H, 3-cyclohexyl-CH); MS (M+1)⁺ *m/z* = 236.3.

4-[[3,5,5-Trimethylcyclohex-2-en-1-ylidene]amino]butanoic acid (19)

¹H NMR (300 MHz, DMSO): δ 1.067 (s, 6H, 5,5-dicyclohexyl-CH₃), 1.321 (s, 2H, 6-cyclohexyl-H), 1.496 (t, 2H, *J* = 3.0 Hz, CH₂ γ to COOH), 1.712–1.758 (m, 2H, CH₂ β to COOH), 1.917 (s, 3H, 3-cyclohexyl-CH₃), 2.090 (s, 2H, 4-cyclohexyl-H), 2.241 (t, 2H, *J* = 7.2 Hz, CH₂ α to COOH), 4.695 (s, 1H, 2-cyclohexyl-H), 10.207 (s, 1H, COOH, D₂O exchangeable); MS (M⁺) *m/z* = 223.0.

4-[[2-Methyl-4-oxocyclohexa-2,5-dien-1-ylidene]amino]butanoic acid (20)

¹H NMR (300 MHz, D₂O): δ 1.258 (t, 2H, *J* = 6.3 Hz, CH₂ γ to COOH), 1.730–1.820 (m, 2H, CH₂ β to COOH), 2.018 (s, 3H, CH₃), 2.190 (t, 2H, *J* = 3.9 Hz, CH₂ α to COOH), 6.495 (d, 1H, *J* = 4.2 Hz, cyclohexyl-CH), 6.600 (d, 1H, *J* = 3.0 Hz, cyclohexyl-CH); MS (M⁺) *m/z* = 206.9.

4-[[1-(Naphthalen-2-yl)ethylidene]amino]butanoic acid (21)

¹H NMR (300 MHz, CDCl₃): δ 0.995 (s, 3H, CH₃), 1.606–1.689 (m, 2H, CH₂ β to COOH), 2.252 (t, 2H, *J* = 8.7 Hz, CH₂ γ to COOH), 3.659–3.690 (t, 2H, *J* = 7.2 Hz, CH₂ α to COOH), 6.956–7.378 (m, 7H, aryl-H), 10.907 (s, 1H, COOH, D₂O exchangeable); MS (M+1)⁺ *m/z* = 256.2.

3-[[2-Ethyl-10-oxo-9,10-dihydroanthracene-9-ylidene]amino]benzoic acid (27)

¹H NMR (300 MHz, CDCl₃): δ 0.833 (t, 3H, *J* = 2.1 Hz, CH₃), 2.698–2.714 (m, 2H, CH₂), 7.2579–8.179 (m, 11H, aryl-H), 11.380 (s, 1H, COOH, D₂O exchangeable); MS (M⁺) *m/z* = 355.5.

3-[[1,4,5,8-Tetrachloro-10-oxo-9,10-dihydroanthracene-9-ylidene]amino]benzoic acid (28)

¹H NMR (300 MHz, DMSO): δ 5.618–7.156 (m, 8H, aryl-H), 11.402 (s, 1H, COOH, D₂O exchangeable); MS (M+1)⁺ *m/z* = 464.2.

3-[[10-Oxo-9,10-dihydrophenanthrene-9-ylidene]amino]benzoic acid (29)

¹H NMR (300 MHz, DMSO): δ 6.909–7.566 (m, 12H, aryl-H), 11.251 (s, 1H, COOH, D₂O exchangeable); MS (M+1)⁺ *m/z* = 328.2.

3-[(10-Oxo-9,10-dihydroanthracene-9-ylidene)amino]benzoic acid (**30**)

^1H NMR (300 MHz, DMSO): δ 7.360–8.688 (m, 12H, aryl-H), 12.108 (s, 1H, COOH, D_2O exchangeable); MS $(\text{M}+1)^+$ m/z = 328.2.

3-[(2,3,5,6-Tetramethyl-4-oxocyclohexa-2,5-dien-1-ylidene)amino]benzoic acid (**31**)

^1H NMR (300 MHz, CDCl_3): δ 1.520 (s, 6H, 2,6-cyclohexyl- CH_3), 1.898 (s, 6H, 3, 5-cyclohexyl- CH_3), 6.898–7.501 (m, 4H, aryl-H), 9.824 (s, 1H, COOH, D_2O exchangeable); MS $(\text{M}+1)^+$ m/z = 284.7.

Fig. 2 Designed GABA analogues

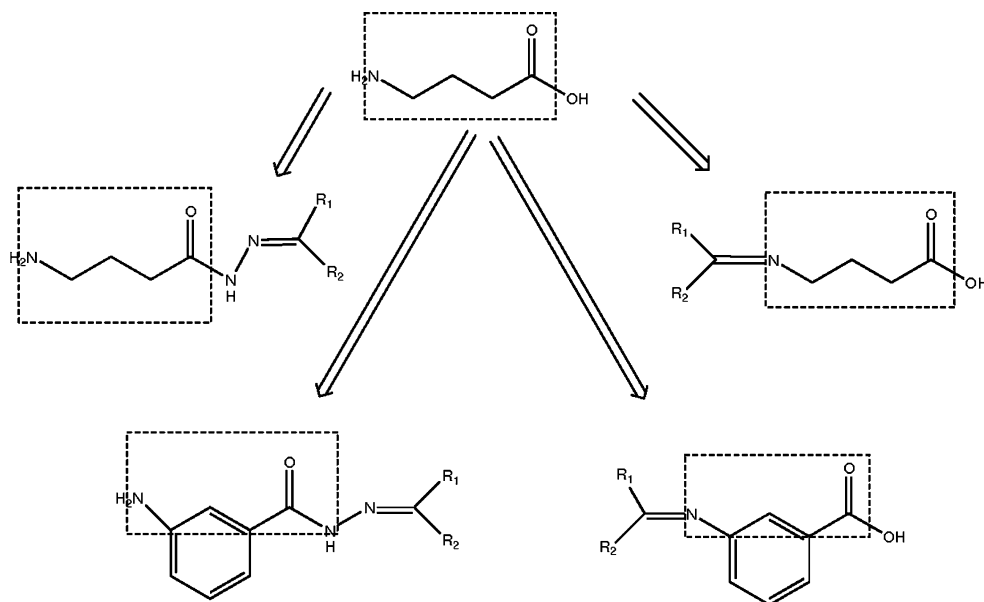
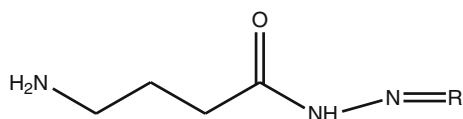


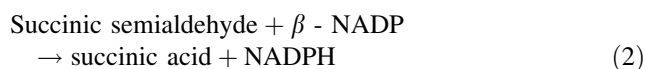
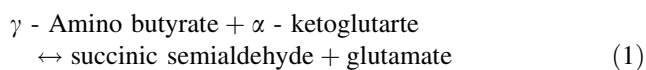
Table 1 Predicted and experimentally determined values of inhibition constant of acid hydrazones of GABA



S. no.	Compound code	R	Observed binding energy (kcal/mol)	Root mean square deviation (RMSD, Å)	Predicted inhibition constant (K_i , μM)	Experimental inhibition constant (IC_{50} , μM)
1.	AHG177	1-(2-Bromophenyl)ethan-1-one	-9.08	25.76	0.221	0.073 ± 0.005
2.	AHG174	1-(3-Chlorophenyl)ethan-1-one	-8.95	26.79	0.277	0.091 ± 0.007
3.	AHG202	2-Methyl-9,10-dihydroanthracene-9,10-dione	-8.88	26.96	0.307	0.11 ± 0.03
4.	AHG066	3-Iodobenzaldehyde	-8.76	25.03	0.376	0.15 ± 0.06
5.	AHG144	1,2,3,4-Tetrahydronaphthalen-2-one	-8.76	24.70	0.376	0.13 ± 0.07
6.	AHG173	9,10-Dihydroanthracene-9,10-dione	-8.74	26.02	0.392	0.14 ± 0.10
7.	AHG063	2-Iodobenzaldehyde	-8.68	24.21	0.433	0.20 ± 0.11
8.	AHG143	1,2,3,4-Tetrahydronaphthalen-1-one	-8.47	25.33	0.614	0.28 ± 0.09
9.	AHG161	1,2-Diphenylethane-1,2-dione	-8.35	27.23	0.752	0.30 ± 0.13
10.	AHG182	4-Bromophenyl(phenyl)methanone	-8.15	23.87	1.050	0.56 ± 0.14

In vitro GABA transaminase activity

The enzymatic activity was determined by coupling the transaminase reaction (Reaction 1) with an excess of SSA dehydrogenase (Reaction 2), so that the formation of reduced pyridine nucleotide is a function of transaminase activity (Scott and Jkoby, 1959; Jakoby, 1962). The reaction was followed spectrophotometrically at 340 nm .



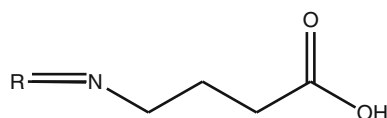
Rat brain GABA-AT was partially purified by the method described by Koo *et al.*, (2003) and Ricci *et al.*, (2006). Enzyme preparation procedures were carried out at 4 °C, unless specified otherwise. The whole brain was isolated, and then homogenized with a glass Teflon homogenizer in four volumes of 0.1 M potassium phosphate buffer (pH 7.4). Homogenate were centrifuged in 600×g for 10 min, supernatant was collected and recentrifuged in 10,000×g for 20 min. Postmitochondrial

fractions were ultracentrifuged in 105,000×g for 1 h, and supernatant was used as enzymatic source in the GABA transaminase assay.

GABA (0.060 M, 0.30 ml), α -ketoglutarate (0.100 M, 0.15 ml), 2-mercaptoethanol (0.100 M, 0.10 ml), potassium pyrophosphate buffer, pH 8.6 (0.100 M, 2.30 ml), tissue homogenate (1 U/ml, 0.02 ml) were incubated in 37 °C for 30 min, followed by the addition of β -NADP (0.025 M, 0.15 ml) and excess of succinic semialdehyde dehydrogenase. The amount of NADPH generated in the brain tissue for 20 min was measured spectrophotometrically at 340 nm using potassium phosphate buffer (0.075 M) and glycerol (25 % v/v) as enzyme dilutor for blank. Increase in A_{340} was observed and recorded. Consecutively, GABA was replaced by synthesized compounds (0.1–100 μ M) and positive control vigabatrin (5–50 μ M) and IC_{50} was determined.

A linear curve of NADPH concentration versus absorbance was obtained at a wavelength of 340 nm. One unit (1 U) of enzyme activity is equivalent to conversion of 1.0 μ mol of GABA to SSA and then to succinate per minute with a stoichiometric reduction of 1.0 μ mol of NADP. Protein concentration was determined by the method of Bradford (1976).

Table 2 Predicted and experimentally determined values of inhibition constant of Schiff's bases of GABA



S. no.	Compound code	R	Observed binding energy (kcal/mol)	Root mean square deviation (RMSD, Å)	Predicted inhibition constant (K_i , μ M)	Experimental inhibition constant (IC_{50} , μ M)
11.	SBG164	1,5-Diphenylpenta-1,4-dien-3-one	−6.12	14.24	32.74	9.95 ± 0.11
12.	SBG195	1-Methyl-9,10-dihydroanthracene-9,10-dione	−6.05	17.10	36.76	–
13.	SBG110	1,3,3-Trimethylbicyclo[2.2.1]heptan-2-one	−5.91	26.03	46.59	10.02 ± 0.08
14.	SBG171	9,10-Dihydrophenanthrene-9,10-dione	−5.83	26.69	53.72	15.53 ± 0.35
15.	SBG211	1,2-Dihydroacenaphthylene-1,2-dione	−5.71	25.70	65.72	16.78 ± 1.03
16.	SBG099	2-Methylcyclohexan-1-one	−5.66	15.20	70.45	20.76 ± 2.46
17.	SBG116	5-Methyl-2-(propan-2-yl)cyclohexan-1-one	−5.66	25.17	70.55	20.82 ± 1.89
18.	SBG120	2-Methyl-5-(prop-1-en-2-yl)cyclohex-2-en-1-one	−5.61	25.18	77.83	23.48 ± 3.02
19.	SBG117	3,5,5-Trimethylcyclohex-2-en-1-one	−5.60	24.42	78.22	25.94 ± 3.55
20.	SBG192	2-Methylcyclohexa-2,5-diene-1,4-dione	−5.59	14.08	79.33	30.12 ± 3.00
21.	SBG153	1-(Naphthalen-2-yl)ethan-1-one	−5.54	15.41	87.49	44.06 ± 5.23

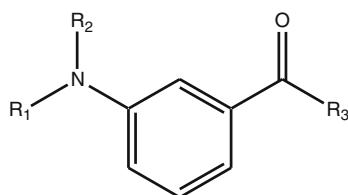
Result and discussion

The design of new and selective inhibitors of an enzyme is one of the most important applications in contemporary rational drug design. A total of 932 GABA derivatives were designed retaining the original structure of GABA, as shown in Fig. 2. To study GABA-AT inhibition, all the designed molecules were docked and the results of LGA docking experiments of different GABA analogs using AutoDock 4.0.1 and AutoGrid 4.0.1 are summarized in Tables 1, 2, and 3. For each docking experiment, the lowest energy docked conformation was selected from 100

runs. The central processing unit for a single docking experiment took 75–120 min, on a 2.19-GHz Intel (R) core2 Duo machine with 2.96 GB of RAM and Red Hat Enterprise Linux 5.0 operating system.

To evaluate accuracy of docking, lower value of binding energy and higher value of inhibition constant (K_i) were set as a criteria for *in silico* screening. 31 flexible docks were considered well docked with the binding energy values < -5.54 kcal/mol (binding energy of vigabatrin). Modeling and docking analysis reveal the nature of the active site and some key interactions that enable the strong binding of acid hydrazones in comparison to Schiff's bases. Docking

Table 3 Predicted and experimentally determined values of inhibition constant of acid hydrazones and schiff's bases of 3-amino benzoic acid



S. no.	Compound code	R ₁	R ₂	R ₃	Observed binding energy (kcal/mol)	Root mean square deviation (RMSD, Å)	Predicted inhibition constant (K_i , μ M)	Experimental inhibition constant (IC_{50} , μ M)
22.	AHABA 199	H	H	10-Hydrazinylidene-7,8-dihydroxy-9,10-dihydroanthracene-9-one	-8.38	24.46	0.72	0.24 \pm 0.03
23.	AHABA 174	H	H	[1-(3-Chlorophenyl)ethylidene] hydrazine	-8.20	26.89	0.98	0.32 \pm 0.02
24.	AHABA 181	H	H	4-Chlorophenyl(phenyl)methylidene] hydrazine	-8.11	22.10	1.13	0.37 \pm 0.01
25.	AHABA 215	H	H	7-Chloro-10-hydrazinylidene-4a,9,9a,10-tetrahydroanthracene-9-one	-8.03	23.54	1.29	0.46 \pm 0.02
26.	AHABA 201	H	H	2,3,5,6-Tetrachloro-4-hydrazinylidene-cyclohexa-2,5-dien-1-one	-7.83	21.25	1.81	-
27.	SBABA 210	2-Ethyl-9,10-dihydroanthracene-9,10-dione		OH	-7.39	25.26	3.86	1.21 \pm 0.06
28.	SBABA 204	1,4,5,8-Tetrachloro-9,10-dihydroanthracene-9,10-dione		OH	-7.36	17.42	4.04	-
29.	SBABA 171	9,10-Dihydrophe-nanthrene-9,10-dione		OH	-6.72	24.77	11.81	2.78 \pm 0.21
30.	SBABA 173	9,10-Dihydroanthracene-9,10-dione		OH	-6.68	25.36	12.78	4.96 \pm 1.01
31.	SBABA 203	2,3,5,6-Tetramethylcyclohexa-2,5-diene-1,4-dione		OH	-6.37	26.05	21.46	6.54 \pm 1.69
32.	Vigabatrin	-		-	-5.54	19.98	86.55	41.21 \pm 3.38

interactions of 4-amino-*N'*-[1-(2-bromophenyl)ethylidene]butanehydrazide (AHG177), 3-amino-*N'*-[1,4-dihydroxy-10-oxo-9,10-dihydroanthracene-9-ylidene]benzohydrazide (AHABA199), 4-[[1,5-diphenylpenta-1,4-dien-3-ylidene]amino]butanoic acid (SBG164), and 3-[[2-ethyl-10-oxo-9,10-dihydroanthracene-9-ylidene]amino]benzoic acid (SBABA210) with Lys 329 appears to be in close proximity and explains the high GABA-AT inhibitory activity observed in their respective series. Docking poses and binding interactions of vigabatrin, AHG177, AHABA199, SBG164, and SBABA210 are shown in Figs. 3, 4, and Table 4. The internal aldimine linkage between Lys-329 and PLP of the enzyme has been broken. Instead, a covalent ternary adduct is formed among the cofactor, the inhibitor, and the lysine residue. The presence of aromatic ring was found to play a major role in determining inhibitory activity for GABA-AT. An amino acid ILE72 and SER74 seems to be in key interactions with ligands.

In order to rationalize the putative binding mode of newly designed compounds, few of them were synthesized as per Schemes 1 and 2 and screened for *in vitro* GABA transaminase inhibitory activity. The biological results were found in agreement with the docking results and are shown in Fig. 5. Incubation of GABA analogs with rat brain aminobutyrate results in a rapid, irreversible, and complete loss of biological activity. The inactivation is progressive with time and follows pseudo-first-order kinetics. Enzymatic half life ranges from 11 to 20 min.

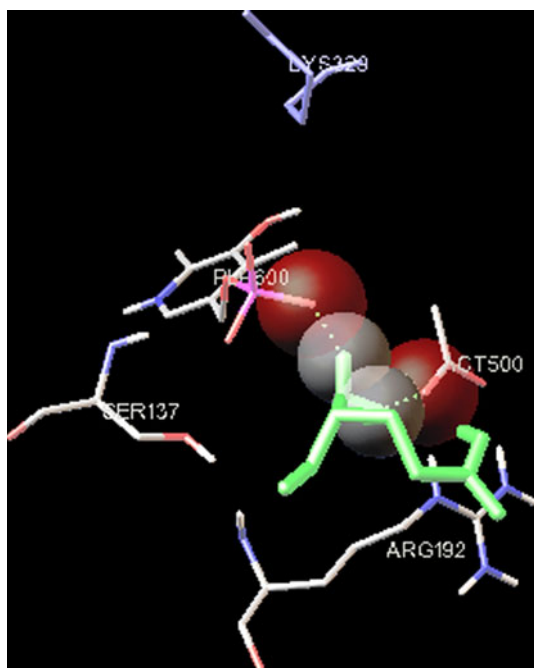


Fig. 3 Docking predicted poses and interactions of vigabatrin with GABA-AT (structure of vigabatrin is displayed in green) (Color figure online)

Only 5–10 % of control activity is restored upon exhaustive dialysis for 4 days, suggesting that the observed inhibition is due to covalent bond formation between the inhibitor and the enzyme.

All the synthesized compounds have been characterized by physicochemical and spectral studies and the data was within accordance of theoretical values. In general, the IR spectra showed $C\equiv N$ peak at $1,620\text{--}1,590\text{ cm}^{-1}$ and characteristic amide bonds at $1,650\text{--}1,630\text{ cm}^{-1}$. The ^1H NMR spectrum revealed that the hydrazino proton ($=N\text{--}NH$) showed a singlet at δ 8.55–10.00. All compounds showed a characteristic D_2O exchangeable signal due to COOH proton of acid function group at δ 11.00–11.55. The aromatic ring proton resonate at δ is $\sim 7.25\text{--}7.6$ ppm.

A discussion of structure–activity relationships of the GABA-AT inhibitors is, at best, tentative. Aminobutyrate transaminase is a pyridoxal-P enzyme which follows a bi–bi ping pong mechanism and in pyridoxamine form can readily transaminate only with SSA and 2-oxoglutarate. The above results strongly suggest that only the pyridoxal form of the enzyme is capable of reacting with the ligands (Fig. 6). The Pharmacophore observed from the ongoing studies is indicated in Fig. 3. The 4-amino-*N'*-[(1Z)-1-(2-bromophenyl)ethylidene]butanehydrazide (AHG177) has been identified as a highly potent inhibitor of the GABA-AT. This compound has displayed significant activity at the inhibitory concentration (IC_{50}) of $0.073\text{ }\mu\text{M}$.

In addition, a number of acid hydrazones have shown to be powerful GABA-AT inhibitors. From these studies, and from related molecular modeling investigations it became apparent that the majority of the inhibitors are closely related to the structure of GABA, as the values of inhibition constant of GABA derivatives was observed higher than 3-aminobenzoic acid derivatives. Moreover, the presence of $-\text{CONH}-$ group and free terminal NH_2 group afforded potent inhibitors. This may be through the hydrogen bond formation. Introduction of acetophenone substituent yielded another agent (AHG174; $\text{IC}_{50} = 0.091\text{ }\mu\text{M}$) with potent GABA-AT enzyme affinity. In these inhibitors, replacement of acetophenone with anthraquinone and benzaldehyde derivatives caused the reduction in potential. Likewise, halogen-substituted analogs inhibited the enzyme more firmly, probably because of higher electronegativity. Introduction of rigidity (decreased number of conformation of methyl chain between amino and carboxyl group) caused the reduction in inhibitory activity.

Replacement of COOH group by CONHN(R1R2) showed variable effects like; (a) R_1 : H or CH_3 and R_2 : 2-bromophenyl, 3-chlorophenyl, 3-iodophenyl, and 2-iodophenyl (in decreasing order of potency); (b) R_1 and R_2 may be collectively replaced by polynuclear aromatic hydrocarbon: 2-methylantraquinone, β -tetralone, anthraquinone, α -tetralone, benzyl, alizarin, benzophenone,

Fig. 4 Docking predicted poses and interactions of AHG177 (a), AHABA199 (b), SBG164 (c), and SBABA210 (d) with GABA-AT (structure of ligands are displayed in green) (Color figure online)

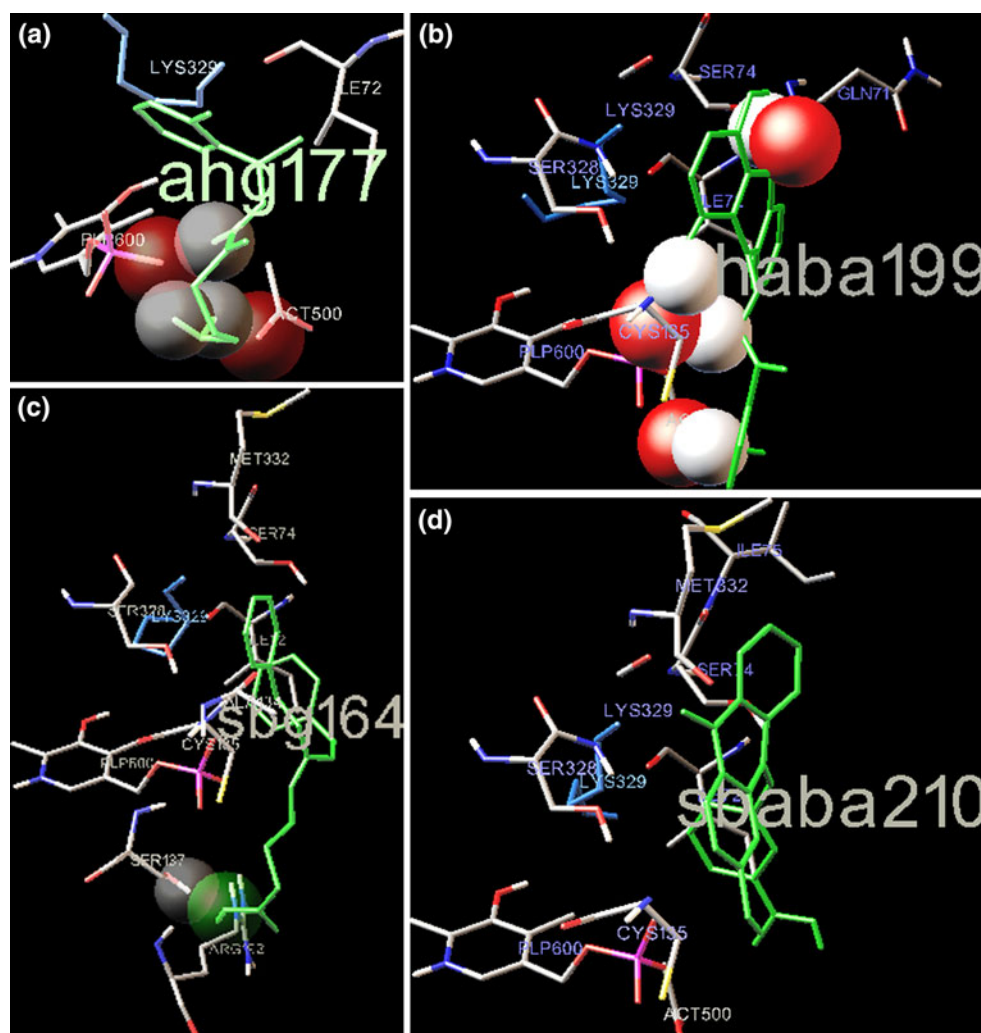
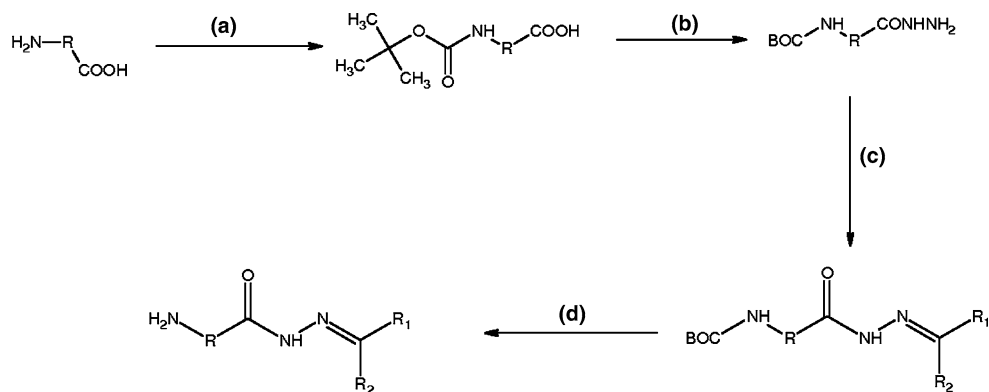


Table 4 Binding interactions of AHG177, AHABA199, SBG164, and SBABA210

Compound	Amino acid in vicinity	Interactions observed
AHG177	ILE72, LYS329, ACT500, and PLP600	Hydrophobic interaction between LYS329 and phenyl group Hydrophobic interaction between ILE72 and CH ₃ of acyl group Hydrogen bonding interactions between PLP600 and amide NH and terminal NH ₂ group Hydrogen bonding interactions between ACT500 and terminal NH ₂ group
AHABA199	GLN71, ILE72, SER74, CYS135, LYS329, ACT500, and PLP600	Hydrogen bonding interactions between SER74 and oxo group of anthraquinone nucleus Hydrogen bonding interactions between PLP600 and amide NH Hydrogen bonding interactions between ACT500 and terminal NH ₂ group
SBG164	ILE72, SER74, ALA 134, CYS135, SER137, ARG192, LYS329, and PLP600	Hydrophobic interaction between ILE72 and phenyl group Hydrogen bonding interactions between SER137 and hydroxyl group of terminal carboxylic group
SBABA210	ILE72, SER74, CYS135, LYS329, ACT500, and PLP600	Hydrophobic interaction between ILE72 and anthraquinone group

Scheme 1 Scheme for the synthesis of **1–10** and **22–26**. *a* Dioxane, water, IM NaOH, BOC (di-*t*-butyl pyrocarbonate); *b* dichloromethane, DCC, $\text{NH}_2\text{NH}_2 \cdot \text{H}_2\text{O}$; *c* EtOH, AcOH, $\text{R}_1\text{CO}\text{R}_2$, reflux; *d* trifluoroacetic acid



Scheme 2 Scheme for the synthesis of **11**, **13–21** and **27–31**. *a* EtOH, H_2SO_4 , reflux; *b* EtOH, AcOH, $\text{R}_1\text{CO}\text{R}_2$, reflux; *c* water, KOH, reflux, dilute H_2SO_4

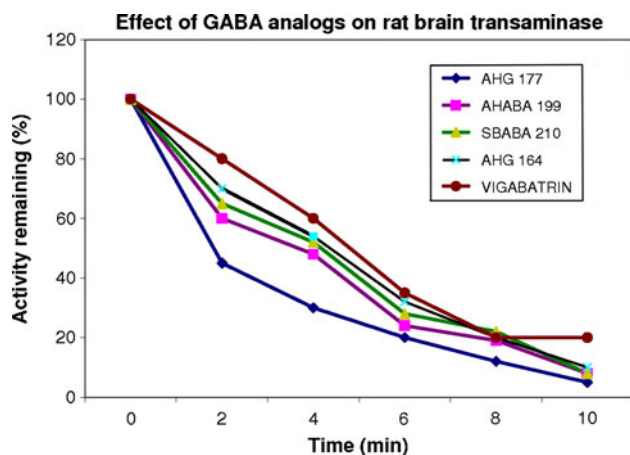
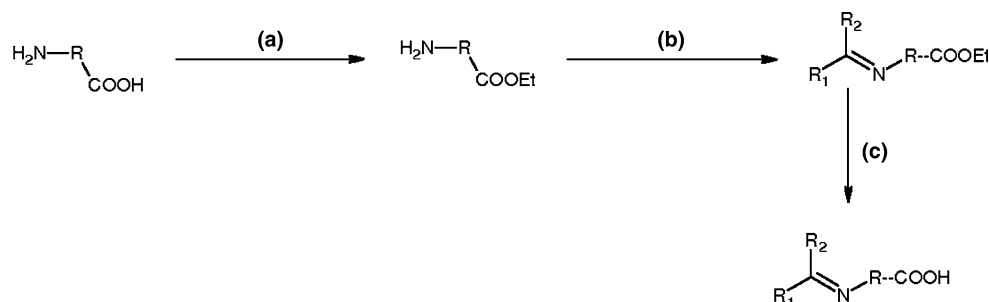


Fig. 5 Effect of GABA analogs on rat brain GABA transaminase

2-chloroanthraquinone, and chloroanil (in decreasing order of potency). Formation of imine link with free NH_2 further reduces the potency in the order: Dibenzylideneacetone, fenchone, 2-methylcyclohexanone, menthone, carvone, and isophorone.

This study contributes molecular insight into the binding process, which is of great pivotal importance for designing new ligands interfering with GABA-AT and shows that new wave of flexible ligand docking program like AutoDock can produce unbiased docking of GABA-AT inhibitors in the enzyme active site. There is still significant

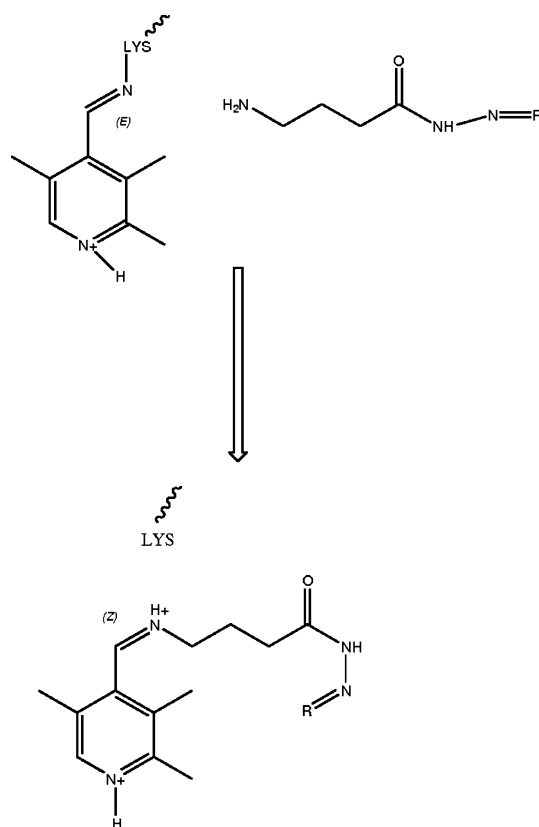


Fig. 6 Proposed mechanism of inhibition of aminobutyrate transaminase with acid hydrazones

room for improvement especially for the empirical binding free energy force field and inhibition constant prediction. Designing and synthesis followed by in vitro interactions provide us important conclusions; decreased number of conformation of methyl chain between amino and carboxyl group, i.e., increase in rigidity causes the reduction in inhibitory activity observed, introduction of halogen atoms especially bromo and chloro significantly improved the activity. Free terminal NH_2 group and $-\text{CONH}-$ group is mandatory for the activity. Thus, our findings open up the possibility to extend this protocol to different databases in order to find new potential inhibitor for promising targets based on a rational drug design process.

Acknowledgments Author wishes to thank Vice Chancellor, Birla Institute of Technology, Mesra, Ranchi and Chairman, Bharat Institute of Technology, Meerut to provide necessary infrastructural and other facilities.

References

- Allison SA, Bacquet RJ, McCammon JA (1998) Simulation of the diffusion-controlled reaction between superoxide and superoxide dismutase II: detailed models. *Biopolymers* 27:251–269
- Bansal SK, Sinha BN, Khosa RL, Olson AJ (2010) Novel GABA-AT inhibitors: QSAR and docking based virtual screening of phenyl-substituted β -phenyl ethylidene hydrazine analogs. *Med Chem Res* 19:S114
- Bansal SK, Sinha BN, Khosa RL (2011a) QSAR and docking-based computational chemistry approach to novel GABA-AT inhibitors: kNN-MFA based 3DQSAR model for phenyl-substituted analogs of β -phenylethylidene hydrazine. *Med Chem Res* 20:549–553
- Bansal SK, Sinha BN, Khosa RL (2011b) Docking based virtual screening of schiff's bases of GABA- a prospective to novel GABA-AT inhibitors. *Med Chem Res*. doi:10.1007/s00044-011-9843-6
- Bansal SK, Sinha BN, Khosa RL, Olson AJ (2011c) Novel GABA-AT inhibitors: QSAR and docking based virtual screening of phenyl-substituted β -phenyl ethylidene hydrazine analogs. *Med Chem Res* 20:1482–1489
- Barbara M (2005) New anticonvulsant agents. *Curr Top Med Chem* 5:69–85
- Bradford MM (1976) Rapid and sensitive method for quantitation of microgram quantities of protein utilizing the principle of dye binding. *Anal Biochem* 72:248–254
- Gasteiger J, Marsili M (1980) Iterative partial equalization of orbital electronegativity—a rapid access to atomic charges. *Tetrahedron* 36:3219–3228
- Gerlach AC, Krajewski JL (2010) Antiepileptic drug discovery and development: what have we learned and where are we going? *Pharmaceuticals* 3:2884–2899
- Goodford PJ (1985) A computational procedure for determining energetically favorable binding sites on biologically important macromolecules. *J Med Chem* 28:849–857
- Goodsell DS, Olson AJ (1990) Automated docking of substrates to proteins by simulated annealing. *Proteins Struct Funct Genet* 8:195–202
- Hardy LW, Abraham DJ, Sapo MK (2003) Structure based drug design. In: Abraham DJ (ed) *Burger's medicinal chemistry and drug discovery*. Wiley, New Jersey
- Jakoby WB (1962) Enzymes of γ -aminobutyrate metabolism. *Methods Enzymol* 5:771–774
- Karlsson A, Fønnum F, Malthe-Sørensen D, Storm-Mathisen J (1974) Effect of convulsive agent 3-mercaptopyruvic acid on the levels of GABA other amino acids and glutamate decarboxylase in different regions of rat brain. *Biochem Pharmacol* 23:3053–3061
- Koo BS, Park KS, Ha JH, Park JH, Lim JC, Lee DU (2003) Inhibitory effects of the fragrance inhalation of essential oil from *Acorus gramineus* on central nervous system. *Biol Pharm Bull* 26:978–982
- Krogsgaard-Larsen P (1981) Gamma-aminobutyric acid agonists antagonists and uptake inhibitors Design and therapeutic aspects. *J Med Chem* 24:1377–1383
- Kwon OS, Park J, Churchich JE (1992) Brain 4-aminobutyrate aminotransferase: isolation and sequence of a cDNA encoding the enzyme. *J Biol Chem* 267:7215–7216
- Morris GM, Goodsell DS, Huey R, Olson AJ (1996) Distributed automated docking of flexible ligands to proteins: parallel applications of Autodock 2.4. *J Comput Aided Mol Des* 10:293–304
- Nogardiy T, Weaver DF (2005) *Medicinal chemistry: a molecular and biochemical approach*. Oxford University Press, New York
- Novikov FN, Chilov GG (2009) Molecular docking: theoretical background, practical applications and perspectives. *Mendeleev Commun* 19:237–242
- Osolodkin DI, Chupakhin VI, Palyulin VA, Zefirov NS (2009) Molecular modeling of ligand-receptor interaction in GABA_C receptor. *J Mol Graph Model* 27:813–821
- Ricci L, Frosini M, Gaggelli N, Valensin G, Machetti F, Sgaragli G, Valoti M (2006) Inhibition of rabbit brain 4-aminobutyrate transaminase by some taurine analogues: a kinetic analysis. *Biochem Pharm* 71:1510–1519
- Scott EM, Jakoby WB (1959) Soluble γ -aminobutyric-glutamic transaminase from *Pseudomonas fluorescens*. *J Biol Chem* 234:932–936
- Sharp K, Fine R, Honig B (1987) Computer simulations of the diffusion of a substrate to an active site of an enzyme. *Science* 236:1460–1463
- Silverman RB, Clift MD (2008) Synthesis and evaluation of novel aromatic substrates and competitive inhibitors of GABA aminotransferase. *Bioorg Med Chem Lett* 18:3122–3125
- Silverman RB, Durkee SC, Invergo BJ (1986) 4-Amino-2-(substituted methyl)-2-butenic acids: substrates and potent inhibitors of gamma-aminobutyric acid aminotransferase. *J Med Chem* 29:764–770
- Smith AJ, Simpson PB (2003) Methodological approaches for the study of GABA_A receptor pharmacology and functional responses. *Anal Bioanal Chem* 377:843–851
- Solis FJ, Wets RJ-B (1981) Minimization by random search techniques. *Math Oper Res* 6:19–30
- Sowa B, Rauw G, Davood A, Fassih A, Knaus EE, Baker GB (2005) Design and biological evaluation of phenyl-substituted analogs of β -phenyl ethylidene hydrazine. *Bioorg Med Chem* 13:4389–4395
- Storici P, Capitani G, Baise DD, Moser M, John RA, Jansonius JN, Schirmer T (1999) Crystal structure of GABA aminotransferase a target for antiepileptic drug therapy. *Biochemistry* 38:8628–8634
- Storici P, Baise DD, Bossa F, Bruno S, Mozzarelli A, Penef C, Silverman RB, Schirmer T (2005) Structure of γ -amino butyric acid (GABA) aminotransferase a pyridoxal 5'-phosphate and [2Fe-2S] cluster-containing enzyme complexed with γ -ethynyl-GABA and with the antiepilepsy drug vigabatrin. *J Biol Chem* 279:363–373
- Toney MD, Pascarella S, Baise DD (1995) Active site model for γ -amino butyrate aminotransferase explains substrate specificity and inhibitor reactivities. *Protein Sci* 4:2366–2374
- Weiner SJ, Kollman PA, Case DA, Singh UC, Ghio C, Alagona G, Profeta S, Weiner P (1984) A new force field for molecular mechanical simulation of nucleic acid and proteins. *J Am Chem Soc* 106:765–784